# DETERMINATION OF DIFFRACTIVE PDFS FROM HERA DATA USING NEURAL NETWORKS IN THE FRAMEWORK OF FRACTURE FUNCTIONS*

Hadi Hashamipour

Istituto Nazionale di Fisica Nucleare, Gruppo Collegato di Cosenza
87036 Arcavacata di Rende, Cosenza, Italy

*Received 13 December 2024, accepted 24 January 2025,*
*published online 6 March 2025*

We present a comprehensive analysis of reduced cross-section data from HERA used to determine diffractive parton distribution functions (DPDFs) using the fracture function formalism. A novel neural network-based methodology is employed, providing an independent determination of DPDFs that is broadly compatible with the previous extractions. This approach improves the flexibility of the QCD analysis, minimizing model-dependent biases, and allowing for a more accurate characterization of diffractive processes.

DOI:10.5506/APhysPolBSupp.18.1-A27

## 1. Introduction

Diffractive deep-inelastic scattering (DIS) processes, characterized by the $ep \to epX$ reaction, with $X$ representing the hadronic final state, have been extensively studied at HERA by the H1 and ZEUS collaborations. These processes, accounting for about 10–15% of all DIS events, provide valuable insights into non-perturbative QCD and the proton's internal structure. Diffractive events are identified via a large rapidity gap (LRG) between the scattered proton and the hadronic system or by detecting the intact proton using forward spectrometers. This unique topology serves as a probe for color-singlet exchange mechanisms in high-energy scattering.

The perturbative QCD (pQCD) factorization theorem allows the diffractive cross section to be factorized into a convolution of DPDFs and calculable hard-scattering coefficients. This enables the study of the partonic structure in diffractive processes, analogous to the study of partonic content in inclusive DIS, with the DGLAP evolution equations describing the scale dependence of the distributions. High-precision HERA data from H1

* Presented at the Diffraction and Low-$x$ 2024 Workshop, Trabia, Palermo, Italy, 8–14 September, 2024.

and ZEUS have significantly enhanced our understanding of diffraction at the parton level, enabling QCD analyses and the extraction of DPDFs with increased accuracy.

In this work, we employ a neural network-based methodology for determining DPDFs within the fracture functions framework [1]. Neural networks provide a flexible, model-independent parameterization, allowing the data to define the shape of the distributions without assuming specific functional forms. Our analysis incorporates the combined and most up-to-date diffractive DIS data from H1 and ZEUS, ensuring a comprehensive and precise determination of DPDFs.

## 2. Theoretical framework

Diffractive DIS processes, represented as $e + p \to e + X + Y$, involve a hadronic system $X$ produced alongside a proton or low-mass excitation $Y$. Key variables in diffractive DIS include photon virtuality ($Q^2$), Bjorken scaling variable ($x$), inelasticity ($y$), squared four-momentum transfer ($t$), diffractive mass ($M_X$), and the longitudinal momentum fraction of the diffractive exchange ($x_{\mathbb{P}}$).

The $t$-integrated cross section for the $ep \to epX$ process is related to the reduced cross section $\sigma_{\mathrm{r}}^{\mathrm{D}(3)}$

$$\frac{\mathrm{d}\sigma_{ep\to epX}}{\mathrm{d}\beta\,\mathrm{d}Q^2\,\mathrm{d}x_{\mathbb{P}}} = \frac{2\pi\alpha^2}{\beta Q^4}\left[1+(1-y)^2\right]\sigma_{\mathrm{r}}^{\mathrm{D}(3)}\left(\beta, Q^2; x_{\mathbb{P}}\right)\,, \tag{1}$$

where $\alpha$ is the fine-structure constant. The reduced cross section $\sigma_{\mathrm{r}}^{\mathrm{D}(3)}$ is decomposed as

$$\sigma_{\mathrm{r}}^{\mathrm{D}(3)}\left(\beta, Q^2, x_{\mathbb{P}}\right) = F_2^{\mathrm{D}(3)}\left(\beta, Q^2, x_{\mathbb{P}}\right) - \frac{y^2}{1+(1-y)^2}F_L^{\mathrm{D}(3)}\left(\beta, Q^2, x_{\mathbb{P}}\right)\,. \tag{2}$$

Using the collinear factorization theorem, the diffractive structure function, $F_k^{\mathrm{D}}(\beta, Q^2, x_{\mathbb{P}}, t)$, $k = 2, L$, is expressed as a convolution of DPDFs $f_{i/p}^{\mathrm{D}}$ and hard-scattering coefficient functions $C_k^i$

$$F_k^{\mathrm{D}}\left(\beta, Q^2, x_{\mathbb{P}}, t\right) = \sum_i \int_\beta^1 \frac{\mathrm{d}\xi}{\xi} f_{i/p}^{\mathrm{D}}\left(\xi, \mu_{\mathrm{F}}^2, x_{\mathbb{P}}, t\right) C_k^i\left(\frac{\beta}{\xi}, \frac{Q^2}{\mu_{\mathrm{F}}^2}, \alpha_{\mathrm{s}}(\mu_{\mathrm{R}})\right)\,. \tag{3}$$

This factorization enables the application of pQCD techniques, similar to inclusive DIS. The fracture functions formalism provides a consistent framework for semi-inclusive DIS processes, where hadrons are produced in the target fragmentation region. Fracture functions $M_{h/i}(x, z, Q^2)$ represent conditional parton densities for observing a specific hadron, addressing factorization challenges in QCD [1–4].

## 3. Methodology

The determination of DPDFs relies on data from the H1 and ZEUS collaborations at HERA, enhanced with measurements from H1 FPS and ZEUS LPS. Combined H1/ZEUS datasets are used to improve statistical precision and reduce systematic uncertainties. To ensure the applicability of pQCD, kinematic cuts are imposed on $\beta$, $M_X$, and $Q^2$, excluding regions where non-perturbative effects dominate. This selection process yields a final dataset of 302 data points, which are used for DPDF parameterization. A feed-forward neural network (NN) is employed for a flexible, model-independent parameterization of the DPDFs. The network, consisting of multiple layers with non-linear activation functions, captures the complex relationships between $\beta$ and the DPDFs. The input to the network is $\beta$, and the output provides the DPDFs at the reference scale $Q_0^2$. The network is trained on reduced cross-section data from HERA, and its weights are optimized by minimizing the $\chi^2$ between the predicted and observed cross sections, allowing the network to map $\beta$ to the DPDFs without predefined functional forms.

To quantify uncertainties in the DPDFs, the Monte Carlo replica method is used. Multiple pseudo-datasets are created by introducing statistical fluctuations in the original data, and each pseudo-dataset is used to train an independent neural network, resulting in an ensemble of networks. The distribution of DPDFs from the ensemble provides a statistical measure of uncertainty. The central value of the DPDFs is the mean of this distribution, and the uncertainty is represented by its standard deviation. This approach ensures the proper propagation of statistical and systematic uncertainties, making the DPDF determination more robust and reliable for further theoretical and experimental analysis.

## 4. Datasets

The study employs inclusive diffractive DIS datasets from the H1 and ZEUS collaborations, including both large rapidity gap and forward proton spectrometer data. The datasets used in our QCD analysis include diffractive DIS data from H1-LRG-11, collected in 2006–2007 with the H1 detector at three center-of-mass energies ($\sqrt{s} = 225$, 252, and 319 GeV) [5], covering $4.0 \leq Q^2 \leq 44.0$ GeV$^2$ and $5 \times 10^{-4} \leq x_{\mathbb{P}} \leq 3 \times 10^{-3}$. Additionally, the H1-LRG-12 dataset, which includes data from 1999–2000 and 2004–2007, extends the kinematic range to $3.5 < Q^2 < 1600$ GeV$^2$ and $0.0003 \leq x_{\mathbb{P}} \leq 0.03$, with constraints on $M_Y < 1.6$ GeV and $|t| < 1$ GeV$^2$ [6, 7]. We also use the H1/ZEUS combined dataset, which consolidates diffractive DIS data from H1 and ZEUS, covering $2.5 < Q^2 < 200$ GeV$^2$, $3.5 \times 10^{-4} < x_{\mathbb{P}} < 0.09$, and $0.09 < |t| < 0.55$ GeV$^2$ [8, 9]. A global normalization factor is applied to account for differences in the range of $t$, assuming an exponential

$t$-dependence with a slope parameter of $b \simeq 6$ GeV$^{-2}$ [9]. The H1/ZEUS dataset is also corrected for proton dissociation using an appropriate global factor [7]. Certain kinematical cuts are applied to the data sets as well, including $Q^2 > 8.5$ GeV$^2$, $\beta \leq 0.8$, $M_X > 2$.

## 5. Results

In this section, we present the results of our DPDFs analysis, determined using the HERA diffractive DIS data and the novel neural network-based methodology described in Section 3. The analysis focuses on obtaining a precise determination of DPDFs at NLO and NNLO accuracy in pQCD, utilizing the fracture functions framework [1–4].

We compared in Fig. 1 the extracted quark and gluon DPDFs with previous sets, such as ZEUS-2010-DPDF [10] and HK19 [4]. The results indicate good agreement with these earlier determinations, particularly for the quark densities. However, the gluon distribution extracted in this work is found to be systematically higher in the intermediate-to-low $\beta$ region compared to the ZEUS-2010-DPDF, which may suggest an improved capability of our approach in fitting the high-precision HERA data. The gluon distribution, however, is very nicely compatible with those of HK19 which used the fracture functions framework. The broader error bands observed in our results may reflect the enhanced flexibility provided by the neural network parameterization, allowing for a more nuanced description of the diffractive parton content.

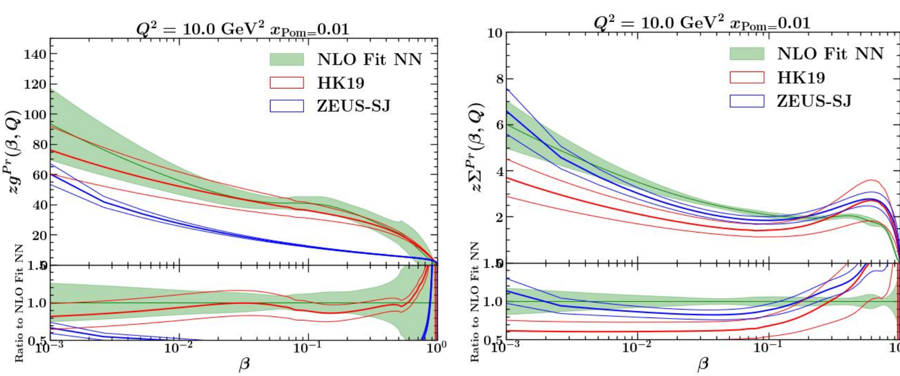


Fig. 1. The diffractive gluon $\beta g(\beta, Q^2, x_{\mathbb{P}})$ and singlet distributions $\beta\Sigma(\beta, Q^2, x_{\mathbb{P}})$ as a function of $\beta$ at $Q^2 = 10$ GeV$^2$ for a selected value of $x_{\mathbb{P}} = 0.01$. The results from ZEUS-2010-DPDF [10] and HK19 [4] are also shown for comparison.

Overall, the extracted gluon and quark densities were found to be compatible with previous determinations. This result highlights the adaptability of the neural network approach, which is capable of capturing subtle features of the diffractive DIS data, particularly in regions of phase space that are less constrained by experimental measurements.

Figure 2 illustrates the comparison between the theoretical prediction calculated using our DPDFs and some selected H1/ZEUS combined datasets. The comparisons are shown for a selected bin of $x_{\mathbb{P}} = 0.05$ for the differ-

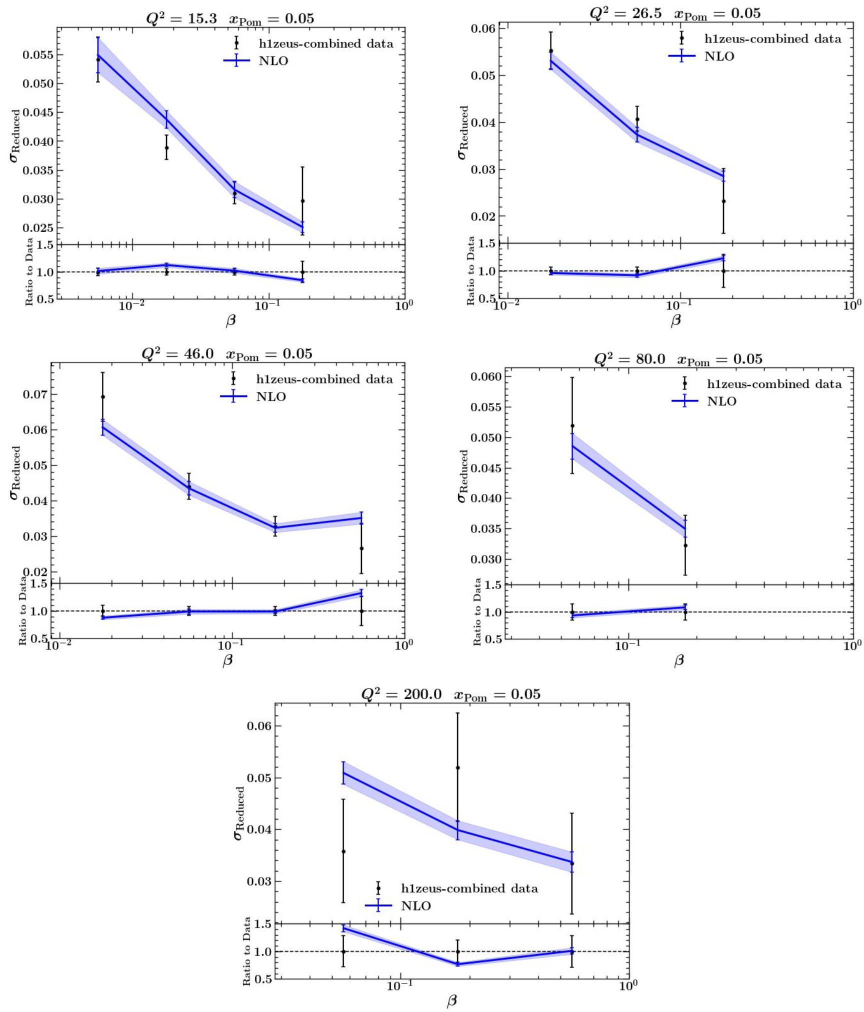


Fig. 2. Comparison between the diffractive DIS data from the H1/ZEUS combined measurements [8] and the corresponding NLO theoretical predictions as a function of $\beta$ using our best-fit NLO DPDFs. The comparisons are shown for a selected bin of $x_{\mathbb{P}} = 0.05$ for the different $Q^2$ values of 15.3, 26.5, 46, 80, and 200 GeV$^2$. We show both the absolute distributions (up panel) and the data/theory ratios (down panel).

ent $Q^2$ values of 15.3, 26.5, 46, 80, and 200 GeV$^2$. As can be seen, the theoretical predictions closely match the experimental measurements for all values of $Q^2$, with data/theory ratios remaining close to unity. This consistency underscores the reliability of the extracted DPDFs in describing the diffractive DIS cross sections. The overall data/theory agreement, particularly for the NLO DPDFs, demonstrates that the extracted distributions provide a robust description of the diffractive DIS data from HERA.

The comparisons shown above demonstrate that the neural network-based DPDFs provide an excellent description of the data across the entire kinematic range considered in this analysis. We expect that the inclusion of NNLO corrections will be particularly effective in improving the agreement with the experimental data, leading to reduced uncertainties in both the gluon and singlet quark distributions.

## 6. Conclusion

The results presented in this work establish a novel approach for the determination of DPDFs, leveraging the fracture function formalism and the flexibility of neural networks to achieve an independent, unbiased extraction. The compatibility with existing datasets, along with the slightly broader distributions obtained, suggests that this method is well-suited for QCD analyses, particularly in environments with high-precision data. Looking ahead, the upcoming EIC will provide an unprecedented opportunity to study diffractive processes with greater accuracy, using both real and simulated pseudo-data to further refine our understanding of the partonic content of the diffraction process.

## REFERENCES

[1] L. Trentadue, G. Veneziano, *Phys. Lett. B* **323**, 201 (1994).
[2] F.A. Ceccopieri, L. Trentadue, *Phys. Lett. B* **655**, 15 (2007).
[3] F.A. Ceccopieri, *Eur. Phys. J. C* **77**, 56 (2017).
[4] H. Khanpour, *Phys. Rev. D* **99**, 054007 (2019).
[5] H1 Collaboration (F.D. Aaron *et al.*), *Eur. Phys. J. C* **71**, 1836 (2011).
[6] H1 Collaboration (F.D. Aaron *et al.*), *Eur. Phys. J. C* **72**, 2074 (2012).
[7] H1 Collaboration (A. Aktas *et al.*), *Eur. Phys. J. C* **48**, 715 (2006).
[8] H1 and ZEUS collaborations (F.D. Aaron *et al.*), *Eur. Phys. J. C* **72**, 2175 (2012).
[9] F.D. Aaron *et al.*, *Eur. Phys. J. C* **71**, 1578 (2011).
[10] ZEUS Collaboration (S. Chekanov *et al.*), *Nucl. Phys. B* **831**, 1 (2010).